Journal of Science and Mathematics Letters, Vol 9, Issue 1, 2021 (77-88)
ISSN 2462-2052, eISSN 2600-8718

RESEARCH PAPER

Effect of Carbonization Temperature on Properties of Char from Palm Kernel Shell

Alhassan Adeku Sallau[1,4]*, Aliyu Jauro[3], Alhaji Modu Kolo[1],
Umar Faruq Hassan[1], Eno Okon Ekanem[2]

[1]Chemistry Department, Abubakar Tafawa Balewa University Bauchi, Bauchi State
[2]Chemistry Department, Federal University Otuoke, Bayelsa State
[3]National Environmental Standards and Regulations Enforcement Agency (NESREA), Abuja
[4]Sheda Science and Technology Complex, Abuja

*Corresponding author: creamysal@yahoo.co.uk

Received: 28 August 2020; Accepted: 11 April 2021; Published: 19 April 2021

To cite this article (APA): Sallau, A. A., Jauro, A., Kolo, A. M., Hassan, U. F., & Ekanem, E. O. (2021). Effect of Carbonization Temperature on Properties of Char from Palm Kernel Shell. *Journal of Science and Mathematics Letters*, *9*(1), 77-88. https://doi.org/10.37134/jsml.vol9.1.7.2021

To link to this article: https://doi.org/10.37134/jsml.vol9.1.7.2021

Abstract

The study investigates the effect of carbonization temperature of palm kernel shell (PKS) biomass, with a view to obtaining char suitable for electrode material. Char were obtained from palm kernel shell by carbonization at temperatures of 600, 800, 1000 and 1150 °C under inert condition for 60 mins each. The effect of carbonization temperature on proximate and ultimate, electrical conductivity, structural and morphological properties was investigated using the ASTM standard method for examination of coal and coke, elemental analyzer, four-point probe, x-ray diffractometer (XRD), Fourier transform infrared (FTIR) spectrometer and scanning electron microscope (SEM). The proximate analysis results showed the char yield to decrease from 29.68 % to 25.27 % as the temperature increases from 600 °C to 1150 °C. While the fixed carbon content in the raw sample was found as 22.22 %, it increases to 73.02 % in char obtained at 600 °C with highest value of 87.45 % obtained at 1150 °C. The volatile matter and moisture content values reduces with increase in temperature. An increase in carbonization temperature, also led to increase in elemental carbon content as well as improved electrical conductivity from 5.56 x 10^{-8} S/cm to 7.67 x 10^{-2} S/cm. Evidence of aromaticity and crystallinity towards graphitization was found from the FTIR and XRD analysis results. The results of electrical conductivity and XRD suggest possible use of the char obtained at 1150 °C for electrode material.

Keywords: Biomass; Carbonization; Correlation; Diffractograms; Morphology; Proximate; Ultimate analysis

INTRODUCTION

Biomass is a promising substitute renewable source to fossil fuels for energy and chemical feedstock with high yield and carbon neutral properties (Wang et al., 2018). The conversion of carbonaceous biomass to carbon using heat is often referred to as carbonization (Daud et al., 2001). Biomass has attracted the research community interest, in an effort to meet the demands of several areas where

energy is much needed, such as in generating electricity, fueling vehicles and heating substances for industrial use (Abdul-Rahman et al., 2016).

Biochar can be used as high-quality fuel, adsorbent, soil amendment, raw material of activation carbon, or even supporter of catalyst and supercapacitor electrodes, etc. (Ma et al., 2017). The composition of the biomass such as cellulose, lignin and hemicellulose and the operational parameters such as final temperature, heating rate and residence time affect the final composition of the char products in terms of its content and characteristic. These two factors interact during thermal degradation of biomass (Rabiu and Zakaria, 2017). Because biomass can provide clean raw feedstock for energy generation, it is safe and economical to turn it into highly sustained value-added bio-products.

Palm kernel shell (PKS) is one of the biomass accruing from oil palm processing, which can be suitably converted to renewable energy material for possible application in energy generation, activated carbon production, catalysis as highlighted earlier. Several studies on PKS characterization, carbonization, pyrolysis and gasification have been reported. In most of these studies; obtaining activated carbon between temperature of 500 to 900 °C was the focus of studies conducted by Ghani et al. (2016); Yashim et al. (2016) and Nicholas et al. (2018). While others investigated the effects of carbonization at temperature of 500 to 700 or 900 °C on the char without activation (Daud et al., 2001; Yang et al., 2006; Okoroigwe and Saffron, 2012; Lee et al., 2017; Wang et al.,2018). To this end, the purpose of the research study is to carbonize PKS at different temperatures of 600, 800, 1000 and 1150 °C; characterize the char products obtained for its proximate, ultimate, structural, morphological, crystalline and electrical properties for possible use in electrode material formulation.

METHODOLOGY

Palm kernel nut was purchased from Kwali market, F.C.T., Abuja, Nigeria. The nut was broken to separate the nut from the shells. The shells were then air dried for 48 hrs, ground and sieved with 2 mm sieve. These were then packed into a stainless steel combustion tube (410 mm long, 34.5 mm inner and 42.5 mm outer diameter) and placed in thermolyte tubular furnace then heated at 600 °C, 800 °C, 1000 °C and 1150 °C temperatures under nitrogen gas atmosphere for 60 mins.

The palm kernel shell and char products were characterized using standard methods of American Society for Testing and Materials (ASTM) method D 4442 – 07 and D1762-84 for the proximate analysis, ultimate analysis was carried out using Perkin Elmer's 2400 Series II CHN Elemental Analyzer, the morphological structure was studied using Phenom ProX scanning electron microscope at central laboratory of the Umar Musa Yar'adua University, Katsina, Nigeria. Functional group was investigated using Thermo Scientific Nicolet iS5 FT-IR Spectrometer at Chemistry Advanced Research Center, Sheda Science and Technology Complex (SHESTCO), Abuja, Nigeria. Crystal structure by Empyrean (panalytical) diffractometer at National geological research laboratory, Kaduna, Nigeria. While the electrical properties were investigated using four-point probe attached to a Keithley source meter (for voltage, current sourcing) and a computer with labtracer 2.0 software for data display.

RESULTS AND DISCUSSION

Proximate analysis and ultimate analysis

The result from the proximate analysis displayed in Table 1, which shows that the raw PKS contains high volatile matter of 70.71 %, fixed carbon of 22.22% and ash content of 3.05%. While 4.02% represent the moisture content. The yield of PKS char corresponding to the temperature treatment of 600 °C, 800 °C, 1000 °C and 1150 °C were 29.69, 28.63, 26.40 and 25.27 respectively, these were slightly similar to 28.57, 28.5 and 27.1 % reported by Yang et al. (2006) for 600, 800 and 1000 °C respectively for similar reaction condition except for the holding time of 30 mins. The decrease in yield may be attributed to the release of more carbon, hydrogen, oxygen from the lignocellulose material of the PKS as the carbonization temperature increases with constant holding time (Daud et al., 2001).

The proximate analysis results of the char obtained at different temperatures showed the moisture and volatile matter content to decrease with increasing temperature as a result of further rapturing of the PKS structural matrix leading to char yield with less moisture and volatile matter. While fixed carbon which is ascribed to the pure carbon form in the char was observed to increase form 73.02 % at 600°C to 87.45 % at 1150°C. The value at 600 °C was similar to 73.26% reported by Wang et al., 2018 for PKS treatment between 400-700°C. This may suggest that increased temperature led to less volatile matter present as a result of been consumed as non-flaking ash leaving relatively pure carbon as fixed carbon (Lee et al., 2017), hence the higher values in fixed carbon. The ash content increases with increasing temperature since the inorganic constituents (mineral elements) are likely less affected by the increasing temperature of carbonization as compared to the organic constituents which continually release oxygen, hydrogen and carbon as a result of bond breaking process which occurs during structural rearrangement (Daud et al., 2001; Lee et al., 2017). Similarly, the results from the ultimate analysis showed that the elemental percentage of carbon increase substantially in all the char obtained at different temperatures.

About 75 % increase was observed for PKS 600, while for PKS 1150, 200 % increase was observed. The result agrees with the report that biochar obtained at higher temperatures (i.e. >500 °C) has a stronger occurrence of C–C bonds compared to C–H and C–O bonds (Nanda et al., 2015), suggesting the formation of highly carbonaceous and aromatic compound (Imam and Capareda, 2012; Kong et al., 2019).

Table 1. Proximate and ultimate analysis carbon material and char products.

	Yield (%)	Proximate analysis (%)				Ultimate analysis (%)					Resistivity ρ (Ω*cm)	Conductivity S/cm
		MC	VM	FC	Ash	C	H	O	N	S		
PKS Raw		4.02	70.71	22.22	3.05	49.63	5.57	43.82	0.44	0.54	-	-
PKS600	29.68	2.63	17.53	73.02	6.82	86.2	4.69	8.85	0.23	0.03	1.80×10^{7}	5.56×10^{-8}
PKS800	28.63	2.20	9.22	81.36	7.22	90.03	3.41	6.48	0.05	0.03	278.01	3.60×10^{-3}
PKS1000	26.40	1.73	4.51	86.52	7.24	94.74	0.61	4.63	0.01	0.01	45.75	2.19×10^{-2}
PKS1150	25.27	1.45	3.83	87.45	7.27	99.56	0.21	0.21	0.01	0.01	13.03	7.67×10^{-2}

Key: MC- moisture content; VM- volatile matter; FC-fixed carbon

Electrical resistance and conductivity

Electrical conductivity (EC) often defined as the reciprocal of electrical resistivity, is considered an intrinsic property of a material which indicates its ability to conduct electric current (Bogeat, 2019). The EC of carbon materials is directly related to their carbon content, precisely with the poly-aromatic carbon content. The poly-aromatic carbon in carbonized biomass are usually organized as

random sheets of graphene, which are directly influenced by the temperature and reaction time of the carbonization process (Hoffmann et al., 2019). The electrical conductivity of a 20mm x 4mm circular disc of PKS char compressed with a force of 10 N, increased from 5.56 x 10^{-8} S/cm at 600 °C to 7.67 x 10^{-2} S/cm at 1150 °C. Though compression force has been shown to influence improved electrical conductivity in bio-carbon materials (Mochidzuki et al., 2003; Bogeat, 2019; Hoffmann et al., 2019). Other factors such as crystallinity, activation, presence of pores have been reported to influence the electrical conductivity as well (Huggins et al., 2014). Thus it is evident that the increase carbonization temperatures led to increased amount of conductive phase in the carbonized PKS by incorporating more carbon atoms into the turbostratic crystallites of the char to form large graphene sheets (Kwon et al., 2013).

FTIR analysis

The FTIR spectra obtained for the raw PKS and char products at different carbonization temperatures is shown in Figure 1. The most observed absorption band in the PKS raw sample are the 3330.37 cm^{-1} broad band peak which is suspected to represent O-H bond from water, alkanols and /or carboxylic fragment. The peaks at 2973.76 cm^{-1} assigned to a methyl C-H asymmetric stretch (Coates, 2019), while that observed at 2382.43 cm^{-1} is assigned C=C stretch of alkyne (Okolo et al., 2020) or C=C stretching of ketone, aldehyde or carboxylic acid group (Chowdhury et al.,2016). The peak at 1736.17 cm^{-1} is due to unconjugated C=O possibly due to uronic anhydride carbonyls and ester groups of carbohydrate, hemicellulose (Ghali et al., 2012) while that 1372.53 cm^{-1} which may be attributed to aliphatic nitro compounds as it is between 1380-1350 cm^{-1} (Nandiyanto et al., 2019) or to O-H group which may also appear between 1395 cm^{-1} and 1360 cm^{-1}, as indication of the presence of the different alcohols and phenols (Yahaya et al., 2020). The peak at 1219.70 cm^{-1} represents the C-O stretching in C-O-H of phenolic group (Liyanage and Pieris, 2015) or deformation of cellulose (Rana et al., 2008). While the peak observed at 1030 cm^{-1} was due to the stretching mode of vibration of C–O of cellulose, hemicelluloses, lignin (Liu et al., 2015 and Satheesh et al., 2019).

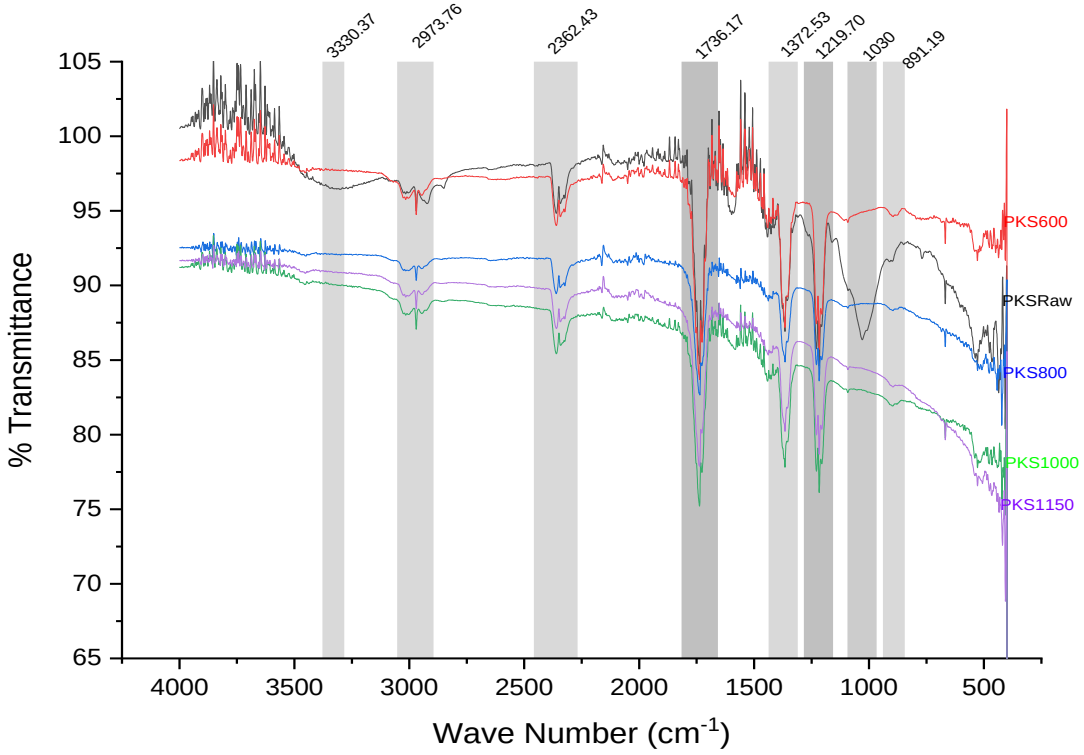

Figure 1. FTIR spectra of PKS and its chars obtained at different temperatures

Similarly, for the PKS char samples, the most observed absorption band in the area are at 2973.76 cm^{-1} assigned to a methyl C-H asymmetric stretch, 2382.43 assigned C=C stretch of alkyne, 1736.17 assigned to unconjugated C=O, 1372.53 to aliphatic nitro compounds or O-H group, 1219.70 cm^{-1} assigned to C-O stretching as explained earlier above. The spectra of char sample suggested structures containing aromatic carbon rings bearing carboxylic phenolic and lactonic groups that contribute to physical adsorption and potentially pseudo-capacitance (Dehkhoda, 2016). The spectra raw data were subjected to principal component analysis (PCA), to detect any subtle differences between the structure of char samples that could not be distinguished visually. As it is common knowledge that PCA is an effective variable reduction technique (Sanguansat, 2012; Liu et al., 2015). In PCA analysis, the samples which appear nearby each other indicates their similarities while those far to each other indicate their differences. This pattern of analysis provides clear discrimination between samples as a tool of identification (Noh et al., 2017). From the PCA results obtained, it was observed that the five samples were highly correlated as shown in Table 2 which were all above 0.5.

Table 2. Correlation for the sample spectra data.

	PKSraw	PKS600	PKS800	PKS1000	PKS1150
PKSraw	1	0.6752	0.46256	0.63534	0.63723
PKS600	0.6752	1	0.87678	0.92788	0.94254
PKS800	0.46256	0.87678	1	0.77336	0.77807
PKS1000	0.63534	0.92788	0.77336	1	0.98837
PKS1150	0.63723	0.94254	0.77807	0.98837	1

The Eigenvalues of the Correlation Matrix displayed in Table 3, showed the first principal components explaining 82.37% of the variance while the second principal components contributed 11.37% and the rest each contribute 5% or less of the total variation.

Table 3. Eigenvalues of the Correlation Matrix

PC	Eigenvalue	Percentage of Variance	Cumulative
1	4.11852	82.37%	82.37%
2	0.56872	11.37%	93.74%
3	0.262	5.24%	98.98%
4	0.04117	0.82%	99.81%
5	0.00959	0.19%	100.00%

In addition, the PC loading plot of Figure 2, showed the PKS-raw well separated and dissimilar to the char products. This reveals that the samples could be distinguished at some degree by the magnitude of carbonization temperature (Reeves, 2012).

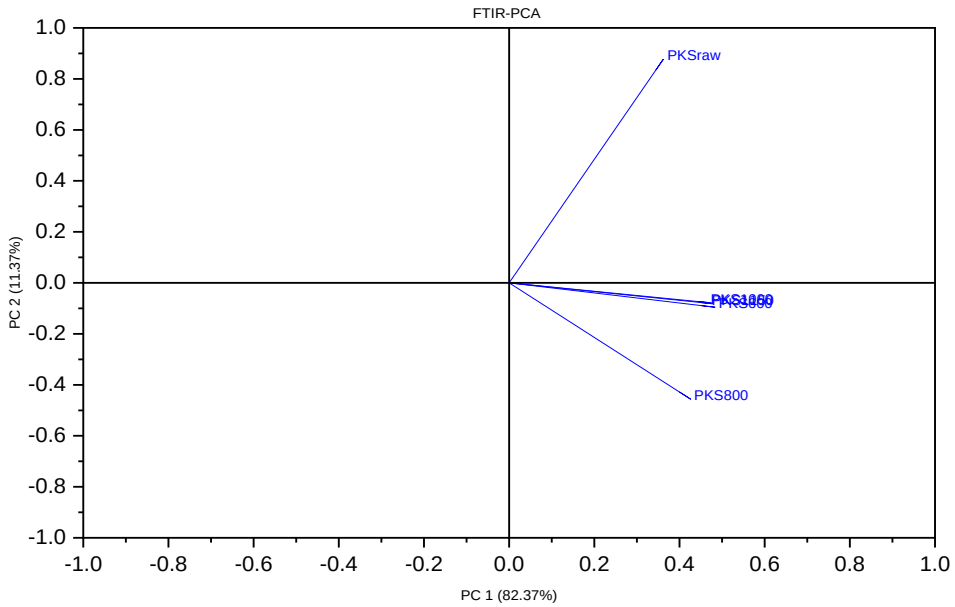

Figure 2. PCA of four char obtained at different temperatures

XRD Analysis

The XRD spectra of PKS and its char at different carbonization temperatures are shown in Figure 3. The diffractograms obtained for appeared similar with progressive development of peaks (002) between 20-25 2theta and peak (100) between 42-47 2theta as the treatment temperature increases. These peaks are commonly attributed to the stacking of the graphitic basal plans of char crystallites (Wang et al., 2018). XRD theory has shown that asymmetric XRD peaks can be found when a sample has a stacked crystal structure or when the sample composition is not uniform. Thus, a carbon material having a graphite structure shows asymmetry of the (002) peak due to stacking defects (Kang et al., 2018).

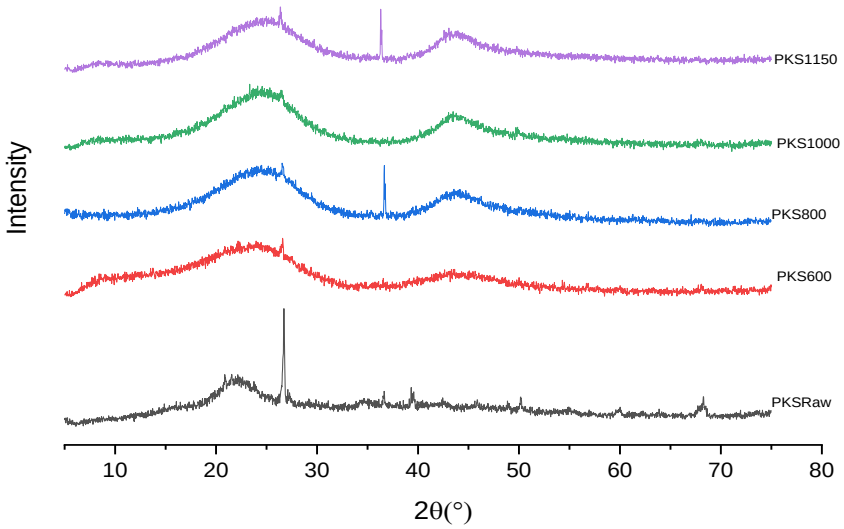

Figure 3. X-ray diffractograms of raw PKS and it char obtained at different temperature

Crystallite geometry in carbon materials parameters such as aromatic layer stacking height (Lc), diameter (La) and inter-layer spacing (d_{002}) are commonly estimated using the Bragg's law and Scherrer equation (Girgis et al., 2007; Stein et al., 2017). Table 4, shows that, as carbonization temperature increases, the value of $d_{(002)}$ decreases from 4.0049 in the raw PKS to 3.5690 Å in PKS1150, whereas that of $d_{(100)}$ decreases from 2.2875 in the raw PKS to 2.0517 Å in PKS1150. The numerical variance of $d_{(002)}$ is greater than that of $d_{(100)}$, which is similar to the results of common carbon materials (Ma et al., 2014; Barnakov et al., 2015). Also, it was noticed that the narrow peak at around 26-27 2theta disappeared as the carbonization temperature increased.

Table 4. Structure parameters of PKS raw and char samples at various temperature.

Sample	d_{002} (Å)	d_{100}(Å)	L_c (Å)	L_c/d_{002}
PKS Raw	4.0049	2.2875	0.894295	0.267913
PKS 600	3.6931	2.0870	0.670859	0.199994
PKS 800	3.6403	2.0701	0.158498	0.043796
PKS 1000	3.6294	2.06053	0.269033	0.076486
PKS 1150	3.5690	2.0517	0.099601	0.028522

The XRD diffractogram were also subjected to PC analysis for detection of similarities and difference in the treatment of PKS char samples as well as possible classification. The result showed the sample to be highly correlated with all values been greater than +0.5. Table 5 showed the details of the strength of linear relationships.

Table 5. Correlation for the sample diffractogram data.

PKSraw	PKS600	PKS800	PKS1000	PKS1150	
PKSraw	1	0.73978	0.76594	0.75714	0.7466
PKS600	0.73978	1	0.91116	0.90825	0.77761
PKS800	0.76594	0.91116	1	0.96115	0.89393
PKS1000	0.75714	0.90825	0.96115	1	0.92792

PKS1150	0.7466	0.77761	0.89393	0.92792	1

The Eigenvalues of the Correlation Matrix displayed in Table 6, showed the first principal components explaining 99.02% of the variance while the rest each contribute less 1% of the total variation.

Table 6. Eigenvalues of the Correlation Matrix.

PC	Eigenvalue	Percentage of Variance	Cumulative
1	4.9508	99.02%	99.02%
2	0.02361	0.47%	99.49%
3	0.01315	0.26%	99.75%
4	0.00996	0.20%	99.95%
5	0.00248	0.05%	100.00%

The PC loading plot displayed in Figure 4, showed the PKS-raw, PKS600 and PKS800 as group of similar variation and different from the group of PKS1000 and PKS1150.

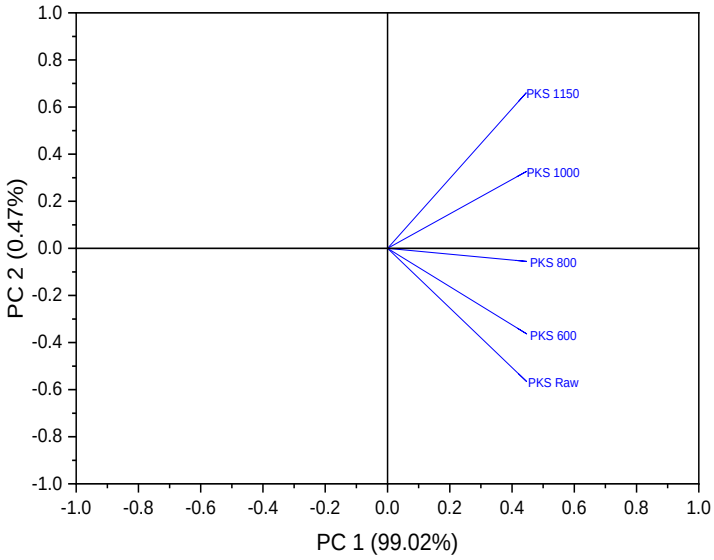

Figure 4. PCA loading plot of the all samples

SEM Analysis

SEM analysis serves as a vital tool for visual observation of changes taking place on the reactive surface of biochar (Štefanko and Leszczynska, 2020) thus the decomposition of hemicellulose, cellulose and lignin during pyrolysis could explain the increase in surface area and pore size of biochar obtained. Scanning electron micrographs of palm shell powder and palm shell char obtained at temperatures 600 ºC, 800 ºC, 1000 °C and 1150 ºC are shown in Figure 5.

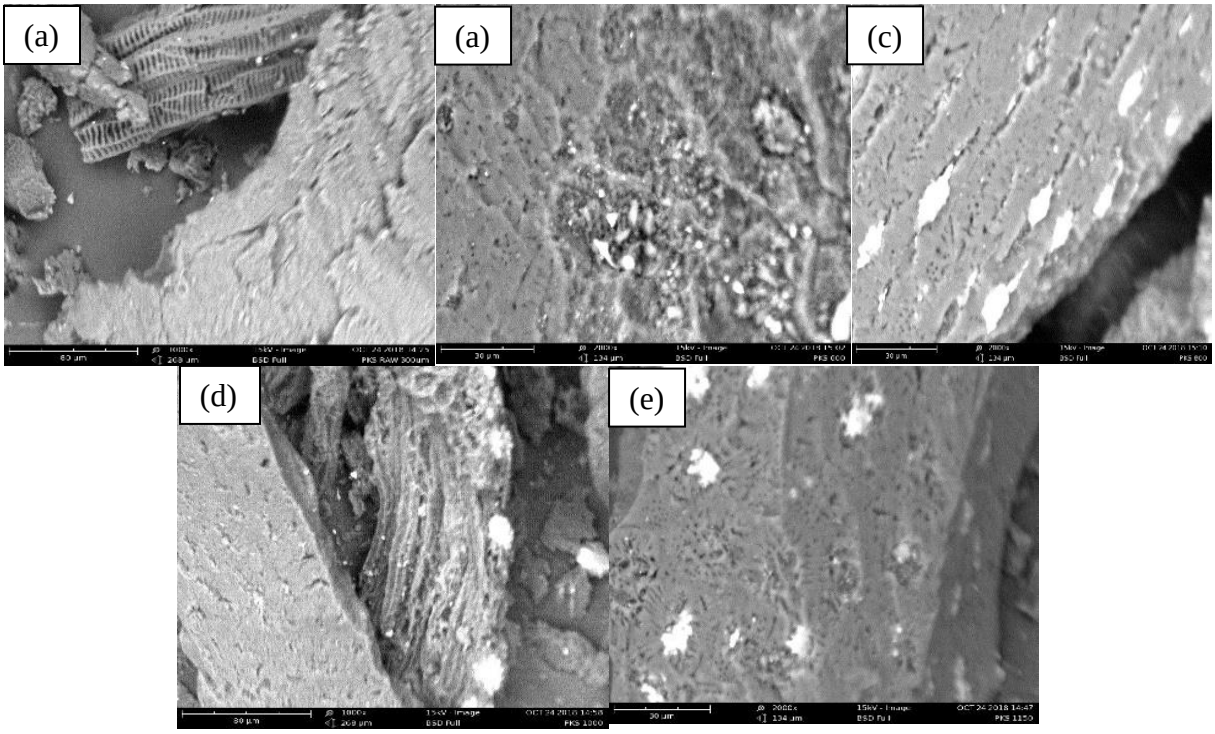

Figure 5. Scanning Electron Microgram of (a) raw PKS and chars obtained at different temperatures of (b) 600 °C, (c) 800 °C, (d) 1000 °C, (e) 1150 °C.

The raw palm shell showed no visible pores at 2000x magnification; however, part of the morphology reveal is a basket-like shape possibly due to fibrous nature of palm kernel waste. The rise in carbonization temperature causes significant transformation to the surface morphology of the chars, as a result of the release of volatiles matter from the PKS samples, which led to the formation of bubbles and pores (Okoroigwea and Saffron, 2012). There are very few pores in the surface of the PKS600 as well as development of crata-like surface. But as the temperature increase to 800 °C more pores and cracks appeared on the surface of PKS800 char. While PKS1000 char exhibits widen pores which extend transversely. The lateral view of the PKS1000 indicate that larger pores are generated internally. This phenomenon is caused by the melting and polymerization of mineral salt at high temperature, leading to the collapse pore wall (Wang et al., 2018). More pores and creta-like structure were noticed on the microgram on PKS1150 °C.

The SEM images for the char samples also revealed the presences of some whitish spots on the biochar surface. These spots maybe due to accumulation of ash minerals and have be suggested to be responsible for blockage of pores on biochar surface (Fernandes et al., 2020). However, the presence of large numbers of pores on the surface of PKS char are regarded as conducive to the movement of electrolyte ions and reduced diffusion resistance (Rout et al., 2016; Ding et al., 2020). This suggest that the increase in carbonization temperature have led to improved PKS char surface.

CONCLUSION

The char properties were found to be highly dependent on the carbonization temperature. As higher temperature treatment promoted a development of more pores. The increase in carbonization temperature led to the formation of char with an aromatic carbon structure and near graphitization

development. Which could greatly improve electrical conductivity and reduce resistance. The results also showed that PKS1150 char had the better properties, in terms of electrical conductivity, SEM and XRD. The PCA results for both FTIR and XRD showed distinction of biochars produced at various temperatures.

ACKNOWLEDGEMENTS

Special appreciation goes to Dr. Abayomi T. O., Dr. Stella A. E., Mr David B. M. at Chemistry Advanced Research Center, and Dr Thomas Imeleria of Advanced Research Center, SHESTCO, Abuja, Nigeria for the support and patient.

REFERENCES

Abdul-Rahman, A., Sulaiman, F. and Abdullah, N. (2016). Influence of Washing Medium Pre-treatment on Pyrolysis Yields and Product Characteristics of Palm Kernel Shell. *Journal of Physical Science. 27(1), 53–75.*

Barnakova, N. C., Khokhlovaa, G. P., Malyshevaa, V. Y., Popovaa, A. N. and Ismagilova, Z. R. (2015). X_Ray Diffraction Analysis of the Crystal Structures of Different Graphite. *Solid Fuel Chemistry. 49(1).,25–29.*

Bogeat, B. A. (2019): Understanding and Tuning the Electrical Conductivity of Activated Carbon: A State-of-the-Art Review, Critical Reviews in Solid State and Materials Sciences. DOI: 10.1080/10408436.2019.1671800

Chowdhury Z. Z., Karim, Z. M., Ashraf, A. M.and Khalid K. (2016). Influence of carbonization temperature on physicochemical properties of biochar derive from slow pyrolysis of Durian wood (Durio zibethinus) sawdust. *Bioresources .11(2),3356-3372.*

Coates, J., (2019). Interpretation of Infrared Spectra, A Practical Approach, Encyclopedia of Analytical Chemistry. Copyrights John Wiley & Sons Ltd.1-23.

Daud, W. M. A. W., Ali, W. S. W. and Sulaiman, Z. M. (2001). Effect of carbonization temperature on the yield and porosity of char produced from palm shell. *Journal of chemical technology and biotechnology. 76.1281-1285.* Doi:10.1002/jctb.515

Dehkhoda, M. A. (2016). Development and characterization of activated biochar as electrode material for capacitive deionization. PhD dissertation (published) Chemical and Biological Engineering, University of British-Columbia, Vancouver.

Ding, Y., Wang, T., Dong, D. and Zhang, Y. (2020). Using biochar and coal as the electrode material for Super capacitor applications. *Frontier Energy Research. 7:159.* Doi:10.3389/fenrg.2019.00159

Fernandes, C. C. B., Mendes, F. K., Júnior, D. F. A., Caldeira, S. P. V., Teófilo, S. M. T, Silva, S. T., Mendonça, V., Souza, F. M. and Silva, V. D. (2020). Impact of Pyrolysis Temperature on the Properties of Eucalyptus Wood-Derived Biochar. *Materials. 13, 5841*.doi:10.3390/ma13245841

Ghali A. E., Marzoug, I. B., Baouab, M. H. V. and Roudesli, M. S. (2012). "Separation and characterization of new cellulosic fibres from the Juncus acutus plant". *Bioresource.7(2). 2002-2018.*

Ghani, W. A.W. K., Fernandez, S. P., Halele, Q. M., Sobri, S. and Jasni, J. (2016). Physical and Electrochemical Characterization of Palm Kernel Shell Biochar (PKSB) as Supercapacitor. MATEC Web of Conferences 62. DOI: 10.1051/matecconf/2016620

Girgis, S. B., Temerk, M. Y., Gadelrab, M. M. and Abdullah, D. I. (2007). X-ray Diffraction Patterns of Activated Carbons Prepared under Various Conditions. *Carbon Science*. *8(2). 95-100.*

Hoffmann, V., Rodriguez, C. C., Sautter, D., Maringolo, E. and Kruse, A. (2019). Study of the electrical conductivity of biobased carbonaceous powder materials under moderate pressure for the application as electrode materials in energy storage technologies. *GCB Bioenergy. 11:230–248.*

Huggins, T., Wanga, H., Kearns, J., Jenkins, P. and Ren, J. Z. (2014). Biochar as a sustainable electrode material for electricity production in microbial fuel cells. *GCB Bioenergy.11:230–248.* https://doi.org/10.1111/gcbb.12545

Imam, T and Capareda, S (2012). Characterization of bio-oil, syn-gas and bio-char from switchgrass pyrolysis at various temperatures. *J. Anal. Appl. Pyrol., 93*: 170-177.

Kang, S. D., Lee, M. S., Lee, H. S. and Roh, S. J. (2018). X-ray diffraction analysis of the crystallinity of phenolic resin-derived carbon as a function of the heating rate during the carbonization process. *Carbon Letters.. 27.108-111.*

Kong, S. H., Loh, K. S., Bachmann, T. R., Zainal, H. and Cheong, Y. K. (2019). Palm kernel shell biochar Production, characteristics and carbon sequestration potential. Journal of Oil Palm Research. DOI:https://doi.org/10.21894/jopr.2019.0041

Kwon, H. J., Park, B. S., Ayrilmis, N., Oh, W. S. and Kim, H. N. (2013). Effect of carbonization temperature on electrical resistivity and physical properties of wood and wood-based composites. *Composites*: *Part B 46, 102–107*. http://dx.doi.org/10.1016/j.compositesb.2012.10.012

Lee, L. C., H'ng, S. P., Paridah, T., Chin, L. K., Khoo, S. P., Nazrin, R. A. R., Asyikin, N. S. and Maminski, M. (2017). Effect of Reaction Time and Temperature on the Properties of Carbon Black Made from Palm Kernel and Coconut Shell. *Asian journal of scientific research. 10 (10). 24-33.*

Liu, Y., He, Z and Uchimiya, M. (2015). Comparison of Biochar Formation from Various Agricultural By-Products Using FTIR Spectroscopy. *Modern Applied Science. 9(4).* www.ccsenet.org/mas

Liyanage D. C. and Pieris, M. (2015). A physico-chemical analysis of coconut shell powder. *Procedia chemistry. 16. 222-228*. www.sciencedirect.com.

Ma, X., Yuan, C. and Liu, X. (2014). Mechanical, Microstructure and Surface Characterizations of Carbon Fibers Prepared from Cellulose after Liquefying and Curing. *Materials 7. 75-84*; doi:10.3390/ma7010075

Ma, Z., Yang, Y., Ma, Q. Zhou, H., Luo, X., Liu, X. and Wang, S. (2017). Evolution of the chemical composition, functional group, pore structure and crystallographic structure of bio-char from palm kernel shell pyrolysis under different temperatures. *Journal of Analytical and Applied Pyrolysis*. http://dx.doi.org/10.1016/j.jaap.2017.07.015

Mochidzuki, K., Soutric, F., Tadokoro, K., Antal, J. M., Toth, M., Zelei, B. and Varhegyi, G. (2003). Electrical and Physical Properties of Carbonized Charcoals. *Ind. Eng. Chem. Res. 42, 5140-5151.*

Nanda, S., Dalai, K. A., Berruti, F. and Kozinski, A. J. (2015). Biochar as an Exceptional Bioresource for Energy, Agronomy, Carbon Sequestration, Activated Carbon and Specialty Materials. *Waste Biomass Valor*. DOI 10.1007/s12649-015-9459-z

Nandiyanto, A. B. D., Oktiani, R. and Ragadhita, R. (2019). How to Read and Interpret FTIR Spectroscope of Organic Material. *Journal of Science & Technology. 4(1).*

Nicholas, F. A., Hussein, Z. M., Zaina, Z. and Khadiran, T. (2018). Palm Kernel Shell Activated Carbon as an Inorganic Framework for Shape-Stabilized Phase Change Material. *Nanomaterials. 8, 689.* doi:10.3390/nano8090689

Noh, C. H. C., Azmin, N. F. M. and Amid, A. (2017). Principal Component Analysis Application on Flavonoids Characterization. *Advances in Science, Technology and Engineering Systems Journal (2) 3, 435-440.*

Okolo, I. B., Oke, O. E., Agu, M. C., Adeyi, O., Nwoso-Obieogu, K. and Akatobi, N. K. (2020). Adsorption of lead(II) from aqueous solution using Africa elemi seed, mucuna shell and oyster shell as adsorbents and optimization using Box–Behnken design. *Applied Water Science. 10:201*. https://doi.org/10.1007/s13201-020-01242-y

Okoroigwea, E. C. and Saffron, C. M. (2012). Determination of bio-energy potential of palm kernel shell by physicochemical Characterization. *Nigerian Journal of Technology (NIJOTECH) 31(3), 329–335.*

Rabiu, Z. and Zakaria, A. Z. (2017). Pyrolignous Acid Production from Palm Kernel Shell Biomass. *J. Appl. Environ. Biol. Sci.*, 7(2S). 59-62.

Rana, R., Mu¨ller, G., Naumann, A. and Polle, A. (2008). FTIR spectroscopy in combination with principal component analysis or cluster analysis as a tool to distinguish beech (*Fagus sylvatica* L.) trees grown at different sites. Holzforschung, 62. 530–538.

Reeves, J. (2012). Mid-infrared spectroscopy of biochars and spectral similarities to coal and kerogens: what are the implications? *Appl. Spectr.. 66:689-695*. http://dx.doi.org/10.1366/11-06478

Rout, T., Pradhan, D., Singh, R. K. and Kumari, N. (2016). Exhaustive study of products obtained from coconut shell Pyrolysis. *J. Environ. Chem. Eng*. http://dx.doi.org/10.1016/j.jece.2016.02.024.

Sanguansat, P. (ed.). (2012). *Principal component analysis - engineering applications.* Intech, Rijeka, Croatia

Satheesh, M., Pugazhvadivu, M., Prabu, B., Gunasegaran, V. and Manikandan, A. (2019). Synthesis and Characterization of Coconut Shell Ash. *Journal of Nanoscience and Nanotechnology. 19, 4123–4128.* www.aspbs.com/jnn

Štefanko, U. A. and Leszczynska, D. (2020). Impact of Biomass Source and Pyrolysis Parameters on Physicochemical Properties of Biochar Manufactured for Innovative Applications. *Frontiers in Energy Research. 8(138), 1-13* doi:10.3389/fenrg.2020.00138

Stein, I.Y., Ashley L. K., Alexander J. C., Luiz A. and Brian L. W. (2017). Mesoscale Evolution of Non-Graphitizing Pyrolytic Carbon in Aligned Carbon Nanotube Carbon Matrix Nanocomposites. *Journal of Materials Science 52(24),13799-13811.*

Wang, P., Zhang, J., Shao, O., Wang, G. (2018). Physicochemical properties evolution of chars from palm kernel shell pyrolysis. *Journal of Thermal Analysis and Calorimetry*. https://doi.org/10.1007/s10973-018-7185-z(0123456789.

Yahaya, Z. A., Somalua, R. M., Muchtara, A., Sulaimanc, A. S. and Dauda, W. R. W. (2020). Effects of temperature on the chemical composition of tars produced from the gasification of coconut and palm kernel shells using downdraft fixed-bed reactor. *Fuel 265*. https://doi.org/10.1016/j.fuel.2019.116910

Yang, H., Yan, R., Chen, H., Lee, H. D., Liang, T. D. and Zheng, C. (2006). Mechanism of Palm Oil Waste Pyrolysis in a Packed Bed. *Energy & Fuels.20, 1321-1328.*

Yashim, M. M., Razali, N., Saadon, N. and Abdul Rahman, N. (2016). Effect of activation temperature on properties of activated carbon prepared from oil palm kernel shell (OPKS). *ARPN Journal of Engineering and Applied Sciences.,11(10), 6389- 6392.*